

Receptor-Mediated Hepatic Uptake of M6P–BSA-Conjugated Triplex-Forming Oligonucleotides in Rats[†]

Zhaoyang Ye,[‡] Kun Cheng,[‡] Ramareddy V. Guntaka,^{*,§} and Ram I. Mahato^{*,‡}

Departments of Pharmaceutical and Molecular Sciences, University of Tennessee Health Science Center, Memphis, Tennessee 38163. Received January 13, 2006; Revised Manuscript Received March 23, 2006

Excessive production of extracellular matrix, predominantly type I collagen, results in liver fibrosis. Earlier we synthesized mannose 6-phosphate–bovine serum albumin (M6P–BSA) and conjugated to the type I collagen specific triplex-forming oligonucleotide (TFO) for its enhanced delivery to hepatic stellate cells (HSCs), which is the principal liver fibrogenic cell. In this report, we demonstrate a time-dependent cellular uptake of M6P–BSA–³³P-TFO by HSC-T6 cells. Both cellular uptake and nuclear deposition of M6P–BSA–³³P-TFO were significantly higher than those of ³³P-TFO, leading to enhanced inhibition of type I collagen transcription. Following systemic administration into rats, hepatic accumulation of M6P–BSA–³³P-TFO increased from 55% to 68% with the number of M6P per BSA from 14 to 27. Unlike ³³P-TFO, there was no significant decrease in the hepatic uptake of (M6P)₂₀–BSA–³³P-TFO in fibrotic rats. Prior administration of excess M6P–BSA decreased the hepatic uptake of (M6P)₂₀–BSA–³³P-TFO from 66% to 40% in normal rats, and from 60% to 15% in fibrotic rats, suggesting M6P/insulin-like growth factor II (M6P/IGF II) receptor-mediated endocytosis of M6P–BSA–³³P-TFO by HSCs. Almost 82% of the total liver uptake in fibrotic rats was contributed by HSCs. In conclusion, by conjugation with M6P–BSA, the TFO could be potentially used for the treatment of liver fibrosis.

INTRODUCTION

Cirrhosis, the advanced stage of liver fibrosis, is the 12th leading cause of medial mortality in 2002 (1). To date, there are no FDA approved antifibrotic drugs (2). Fibrosis is characterized by excessive production of extracellular matrix (ECM) components, especially type I and III fibrillar collagens within the perivascular and interstitial space of tissues (3, 4). Although multiple liver cell types, including periportal and pericentral fibroblasts, produce collagen and lead to liver fibrosis, hepatic stellate cells (HSCs, also known as lipocytes, Ito cells, and perisinusoidal cells) have attracted the most attention (5). HSCs are distributed throughout the hepatic lobule and serve as the principal storage sites for vitamin A. Upon liver injury, infiltrating leukocytes (neutrophils, lymphocytes, and monocytes) along with resident macrophages (Kupffer cells) release various inflammatory cytokines and growth factors, leading to activation of quiescent HSCs into actively proliferating α -smooth muscle actin (α -SMA) positive myofibroblast-like cells (2, 6).

Directly inhibiting the type I collagen synthesis by HSCs is a potential way to prevent liver fibrosis (7). Expression of type α 1(I) collagen gene is regulated at the transcriptional and posttranscriptional level, producing an increase in the mRNA steady-state levels by 60–70-fold in activated HSCs compared with quiescent HSCs (8). Mammalian α 1(I) collagen gene promoter contains two contiguous 30 bp polypurine tracts C1 and C2, located at –141 to –170 and –171 to –200 upstream from the transcription start site (9). Earlier we developed a

triplex-forming oligonucleotide (TFO), which can form a stable triplex with the target gene sequence and inhibit the transcription of rat type α 1(I) collagen gene in vitro. Therefore, this TFO molecule is a potential candidate for treating liver fibrosis.

Following systemic administration, oligonucleotides (ODNs) widely distribute throughout the body with higher uptake in the liver and kidney (10–12). There are several reports on targeted delivery of ODNs to hepatocytes, Kupffer cells, and liver endothelial cells (13–15). We have tested the in vivo distribution of the TFO molecules in normal and fibrotic rats (16). Almost 45% of the injected dose was deposited in the liver in normal rats, but only 35% of injected dose in fibrotic rats. The intrahepatic distribution was nonspecific, with Kupffer and endothelial cells contributing 40% of total liver uptake, HSCs contributing 40%, and hepatocytes 20%.

HSCs comprise only 5–15% of all the liver cells (17). Mannose 6-phosphate/insulin like growth factor II (M6P/IGF II) receptor is expressed on HSCs, and its expression is up-regulated upon activation of these cells due to acute or chronic liver injury (18, 19). To maximize TFO delivery to the liver in general and to HSCs in particular, we recently synthesized mannose 6-phosphate–bovine serum albumin (M6P–BSA) and conjugated to type α 1(I) collagen gene promoter specific TFO via a disulfide bond (37). Following tail vein injection into normal rats, (M6P)₂₀–BSA–³³P-TFO rapidly cleared from the circulation and accumulated mainly in the liver. TFO concentration residing in the HSCs was shown to be much higher with (M6P)₂₀–BSA–³³P-TFO than that with ³³P-TFO (1093 vs 215 ng/mg cell protein).

In the present study, we determined the cellular and nuclear uptake of (M6P)₂₀–BSA–³³P-TFO by HSC-T6 cells, which is an immortalized rat hepatic cell line. The effect of M6P–BSA–TFO on type α 1(I) collagen gene transcription has also been determined by real time RT-PCR. We then determined the effect of number of M6P in M6P–BSA–TFO on biodistribution and hepatic uptake of M6P–BSA–³³P-TFO as well as the intrahepatic distribution after intravenous administration into both

[†] This work was supported by Grant RO1 DK064633 from the NIH and USPHS Grant 47379.

* Corresponding authors. R.I.M.: 26 S Dunlap Street, Room 413, Memphis, TN 38163; tel, (901) 448-6929; fax, (901) 448-6092; e-mail, rmahato@utmem.edu. R.V.G.: 101 Molecular Science Bldg., Memphis, TN 38163; tel, (901) 448-8230; fax, (901) 448-8462; e-mail, rguntaka@utmem.edu.

[‡] Department of Pharmaceutical Sciences.

[§] Department of Molecular Sciences.

normal and fibrotic rats. Subcellular distribution of M6P-BSA-³³P-TFO in nuclei and cytoplasm of the liver cells was also determined at 30 min and 4 h post intravenous injection in rats.

MATERIALS AND METHODS

Materials. Bovine serum albumin (BSA) (fraction V, purity > 98%) was purchased from USB Corporation (Cleveland, OH). *p*-Nitrophenyl- α -D-mannopyranoside (pnpM), phosphorous oxide chloride, palladium (10 wt % on activated carbon), thiophosgene, 0.04% trypan blue, dimethylnitrosamine (DMN), deoxyribonuclease 1 (DNase 1) and Pronase were purchased from Sigma-Aldrich (St. Louis, MO). RNA STAT 60 reagent was purchased from Ambion RNA Diagnostics (Austin, TX). MultiScribe reverse transcriptase reagent was from Applied Biosystems Inc. (Branchburg, NJ). SYBR Green-1 dye universal master mix was from Applied Biosystems Inc. (Foster, CA). [γ -³³P]dATP was purchased from MP Biomedicals (Irvine, CA), and T4 polynucleotide kinase was from New England Biolabs (Beverly, MA). Soluene-350 (tissue solubilizer) and Hionic Fluor (scintillation fluid) were purchased from Perkin-Elmer (Boston, MA). Hydrogen peroxide (H₂O₂) was purchased from Fisher Chemical (Fair Lawn, NJ). Heparin was purchased from American Pharmaceutical Partners, Inc. (Los Angeles, CA). Dulbecco's modified Eagle's medium (DMEM), penicillin G (5000 unit/mL), streptomycin sulfate (5000 μ g/mL), Trypsin-EDTA, and type IV collagenase were from Invitrogen Life Technologies (Carlsbad, CA). Heat-inactivated fetal bovine serum (FBS) was purchased from Atlanta Biologicals (Lawrenceville, GA). Ca²⁺/Mg²⁺-free Hanks balanced salt solution and phenol red free Hanks balanced salt solution (Cellgro) were purchased from MediaTech (Washington, DC). Isoflurane was purchased from Baxter Pharmaceutical Products, Inc. (Deerfield, IL). Nycodenz AG was purchased from Greiner Bio-One, Inc. (Longwood, FL). All solvents and other chemicals used in this study were used as available without further treatment.

TFO, which was a 25 mer antiparallel fully phosphothioate ODN (3'-GAG GGG GGA GGA GGG AAA GGA AGG G-5') targeting α 1(I) collagen gene promoter of rats, was synthesized by The Midland Certified Reagent Company, Inc. (Midland, Texas), and the same TFO modified with a sulfhydryl group at the 3' end (MW: 8684 Da) was synthesized by Invitrogen Life Technologies (Carlsbad, CA).

Synthesis and Characterization of M6P-BSA-TFO. We synthesized M6P-BSA and conjugated it to TFO via a disulfide bond formation as described in our recently published paper (37). Briefly, *p*-nitrophenyl- α -D-mannopyranoside (pnpM) (0.3 g, 1 mmol) was phosphorylated at the 6 position by reacting with phosphorous oxide chloride (0.4 mL, 4.4 mmol) in pyridine (0.4 mL, 5 mmol), acetonitrile (1 mL, 19 mmol), and water (0.04 mL, 2.2 mmol) for 1 h on an ice-water bath to give *p*-nitrophenyl-6-phospho- α -D-mannopyranoside (pnpM6P). PnpM6P (0.25 g, 0.66 mmol) was reduced with 100 mg of 10% palladium on activated carbon under H₂ (1 atm) in 20 mL of a 4:1 (v/v) methanol-water mixture for 2 h to give *p*-aminophenyl-6-phospho- α -D-mannopyranoside (papM6P). Thiophosgene (55 μ L, 0.73 mmol) in 10 mL of chloroform was added to papM6P (50 mg, 0.14 mmol) in 10 mL of 0.1 M sodium carbonate buffer, pH 8.6, and the mixture was vigorously stirred for 1 h to give *p*-isothiocyanatophenyl-6-phospho- α -D-mannopyranoside (itcM6P). ItcM6P (26–75 mg) in 2.0 mL of 0.1 M sodium carbonate buffer, pH 9, and 0.15 M NaCl was added to 30 mg (0.45 μ mol) of BSA in 2.0 mL of the same buffer. The reaction mixture was kept at room temperature for 18 h with stirring and then applied to a PD-10 column. All the intermediate products were verified with ¹H NMR and ESI-MS. The conjugates were verified on 8% sodium dodecyl sulfate-polyacrylamide gel electrophoresis (SDS-PAGE). To have activated disulfide

bonds for conjugation with TFOs, 20 mg of BSA or M6P-BSA was dissolved in 1 mL of 0.1 M sodium borate buffer, pH 8.6 and *N*-succinimidyl 3-(2-pyridyldithio)-propionate (SPDP) (4 mg; 12.8 μ mol) in 0.65 mL of ethanol and the mixture was stirred for 20 h at room temperature. The products were purified on a PD-10 column. The sugar content and number of PDP groups coupled to M6P-BSA or BSA were determined as described previously. TFO modified with sulfhydryl group at the 3' end was first treated with DTT to generate a 3'-thiol functional group and then reacted with 2.5 mg of (M6P)₂₀-BSA-PDP in glycine buffer. The product was eluted with PBS on a G75 column (1 \times 25 cm). The formation of (BSA)₂₀-M6P-TFO conjugate was verified by electrophoresis on a 20% native polyacrylamide gel at room temperature. We obtained M6P-BSA-TFO with different numbers of M6P residues (14, 20, or 27) by altering the molar ratio of itcM6P and BSA. There was one TFO molecule conjugated to M6P-BSA based on the chromatography on a G75 column. TFO was labeled by adding γ -³³P to the 5'-end using [γ -³³P]-ATP and T4 polynucleotide kinase as described (16).

Uptake of M6P-BSA-³³P-TFO by HSC-T6 Cells. Immortalized rat liver stellate cells (HSC-T6) (kindly provided by Dr. Friedman, SL, Mount Sinai School of Medicine, New York, NY) were seeded in 6-well plates at a density of 3.5 \times 10⁵ cells/well in 2 mL of DMEM supplemented with 10% FBS, penicillin G (100 units/ml) and streptomycin sulfate (100 μ g/mL). After 24 h of incubation, the medium was removed and incubated with 1 mL of DMEM containing ³³P-TFO or (M6P)₁₄-BSA-³³P-TFO, (M6P)₂₀-BSA-³³P-TFO, and (M6P)₂₇-BSA-³³P-TFO (3 \times 10⁴ cpm, 0.4 μ M) at 37 °C. The cells were harvested at different time points (5, 20, 70, 120, 180, 240, 300, and 330 min) by removing the medium, washing with ice-cold PBS three times, and trypsinization. Cell pellets were digested with Soluene-350 for 4 h at 55 °C and then overnight at room temperature. After neutralization with H₂O₂, Hionic Fluor was added and the radioactivity was counted using a liquid scintillation counter. Total cellular protein was measured by BCA assay. The TFO concentration was expressed in terms of ng of TFO/ μ g of cell protein.

Polyacrylamide Gel Electrophoresis. To determine the amount of intact TFO taken up by HSC-T6 cells, 3.5 \times 10⁵ cells/well were incubated with ³³P-TFO or (M6P)₂₀-BSA-³³P-TFO (2 \times 10⁵ cpm, 0.4 μ M) at 37 °C for up to 24 h. Cells were harvested at 0.5, 1, 2, 4, 8, 12, and 24 h. The cell pellet was lysed with 500 μ L of 1% SDS lysis buffer (10 mM Tris-HCl, pH 7.4, 150 mM NaCl, and 1% sodium dodecyl sulfate) at 37 °C for 1 h. The lysate was centrifuged at 12000g for 10 min, the supernatant was collected and extracted with an equal volume of phenol/chloroform (v/v, 1/1), the extract was centrifuged for 5 min at 12000g, and the supernatant was collected in microcentrifuge tubes. TFO was precipitated by adding sodium acetate to 0.3 M and a 3-fold volume of 100% ethanol and keeping at -20 °C overnight. The solution was centrifuged at 12000g for 30 min, the supernatant was removed, and the precipitate was air-dried. The TFO pellet was redissolved in 20 μ L of distilled water and analyzed by gel electrophoresis using a 20% polyacrylamide gel at 80 V for 2 h. The gel was autoradiographed for 2 days at 4 °C.

Isolation of Nuclei from HSC-T6 Cells. HSC-T6 cells (5 \times 10⁵ cells/well) were cultured in 6-well plates until 80% confluence. Then, (M6P)₂₀-BSA-³³P-TFO or ³³P-TFO (~1.0 \times 10⁵ cpm, 0.4 μ M) was added in 1 mL of DMEM media in the absence of FBS. At 4 h incubation at 37 °C, the cells were harvested and the nuclei were isolated from cytoplasm using Nuclei EZ PREP nuclei isolation kit (Sigma, St. Louis, MO) following the supplier's protocol. The purity and number of isolated nuclei was determined under microscopy by trypan blue

assay. Isolated nuclei and cytoplasm fraction were digested with Soluene-350 overnight. Hionic Fluor was added and the radioactivity was determined using a liquid scintillation counter. The percentage of nuclear uptake of the TFO was calculated as % of total cellular uptake.

Inhibition of Transcription in HSC-T6 Cells. HSC-T6 cells (5×10^5 cells/well) were cultured in 6-well plates until 70% confluence in DMEM containing 10% of FBS. The media were replaced with 1 mL of FBS-free DMEM containing TFO at a concentration of 0.5 μM or (M6P)₂₀-BSA-TFO at TFO concentrations of 0.2, 0.5, and 1 μM and incubated for 24 h at 37 °C. Cells treated with 1 mL of FBS-free DMEM were used as control. Then an additional 1 mL of DMEM containing 20% of FBS was added, and cells were incubated for another 24 h.

Cells were harvested and total RNA was isolated using RNA STAT 60 reagent. Total RNA (1 μg) was treated with DNase I and then converted to cDNA using MultiScribe reverse transcriptase reagent and random hexamers. One hundred nanograms of the cDNA was amplified by real time PCR using SYBR Green-1 dye universal master mix on ABI Prism 7700 Sequence Detection System. The forward primer specific for type $\alpha 1(\text{I})$ collagen mRNA was 5'-TGGTCCCAAAGGTTCTCCTGGT-3', and the reverse primer 5'-TTAGTCCAGGGAATCCCACACA-3'. The forward and reverse primers specific for type $\alpha 1(\text{I})$ collagen primary mRNA were 5'-CCAGCCGCAAA-GAGTCTACATGTC-3' and 5'-TCACCTTCTCATCCCTCCTAA-3', respectively. The PCR product is 234 bp. Primers (forward, 5'-GTCTGTGATGCCCTTAGATG-3', and reverse, 5'-AGCTTATGACCCGCACTTAC-3') specific for 18S ribosomal RNA were used as internal control for real time PCR. To confirm PCR specificity, the PCR products were subjected to a melting-curve analysis and agarose gel electrophoresis. Relative transcript levels were normalized to 18S rRNA genes. For comparison, transcript levels of control cells were set as 1 and experimental data are shown as fold decrease of control.

Induction of Liver Fibrosis. Dimethylnitrosamine (DMN) induced liver fibrosis in rats has been shown to have a pathology closely resembling that of human cirrhosis (20). Male Sprague-Dawley rats weighing 120–140 g (Harlan Co., San Diego, CA) were housed individually under controlled light (12/12 h) and temperature conditions and had free access to food and water. To induce liver fibrosis, DMN was injected intraperitoneally into rats at a dose of 10 mg/kg of body weight. Injections were given on the first three consecutive days of each week over a 4-week period. After the DMN injection for 4 weeks, 3 rats were killed for examination for liver fibrosis development and measurement of hydroxyproline content (21).

Biodistribution of M6P-BSA-³³P-TFO. The protocol of animal use and care was approved by the Comparative Department of the University of Tennessee Health Science Center. Male Sprague-Dawley rats weighing 150–170 g were anesthetized by inhalation of isoflurane, and then 250 μL of ³³P-TFO or (M6P)₂₀-BSA-³³P-TFO in saline ($\sim 2.2 \times 10^5$ cpm) was injected intravenously into rats at a dose of 0.2 mg of TFO/kg of body weight. After 30 min postinjection, blood (0.2–0.3 mL) was collected by cardiac puncture in heparinized tubes, and urine was also collected directly from the urinary bladder using a 26-gauge needle syringe. Major organs, such as liver, spleen, kidney, lung, heart, and muscle, were isolated, washed with saline, blotted dry, weighed, and stored at -86 °C. Blood was centrifuged, and plasma was separated. One hundred fifty microliters of plasma or 150–200 g of each tissue was incubated with 2 mL of solubilizer Soluene-350 for 3 h at 55 °C first and then overnight at room temperature. Two hundred microliters of 30% H₂O₂ was added to each sample, and each sample was incubated for another 30 min. Ten milliliters of Hionic Fluor scintillation fluid was added to each tissue, plasma, and urine

sample, and the radioactivity of each sample was measured using a scintillation counter.

Competition in Hepatic Uptake of M6P-BSA-³³P-TFO. One minute before the injection of M6P-BSA-³³P-TFO at a dose of 0.2 mg/kg (specific activity: 1×10^6 cpm/mL), rats received 10 mg/kg of M6P-BSA. At 30 min postinjection, blood and urine were collected; other major organs were harvested as described above for radioactivity measurement.

Hepatic Cellular and Subcellular Distribution. To determine the effect of M6P on the hepatic uptake of TFOs by parenchymal cells (hepatocytes) and nonparenchymal cells (Kupffer, endothelial, and Stellate cells), the liver was perfused in situ after intravenous administration of ³³P-TFO or (M6P)₂₀-BSA-³³P-TFO (2×10^5 cpm) at a dose of 0.2 mg of TFO/kg of body weight as described before (37). Briefly, at 30 min postadministration, rats were anesthetized, 100 units of heparin was injected, the abdomen was opened, and the portal vein was cannulated with a PE-60 polyethylene tube. The liver was then perfused with 200 mL of Ca²⁺/Mg²⁺-free Hanks balanced salt solution and then with Hanks balanced salt solution containing 0.05% type IV collagenase and 0.1% Pronase for an additional 250 mL. All the perfusion solutions were incubated at 37 °C. After perfusion, different liver cell types were separated and radioactivity was measured as described before (16). The contributions of various cell types to the total liver uptake were calculated as % of total hepatic uptake.

To isolate nuclei from the whole liver cells, the livers were collected at 30 min or 4 h postinjection of ³³P-TFO or (M6P)₂₀-BSA-³³P-TFO (4×10^5 cpm) at a dose of 0.2 mg of TFO/kg of body weight, washed, and blotted dry. One gram of fresh liver tissue was used for isolation of nuclei using Nuclei PURE Prep nuclei isolation kit according to the supplier's protocol (Sigma-Aldrich, St Louis, MO). The purity and number of isolated nuclei were determined under microscopy by dilution in trypan blue solution. The yield of nuclei was calculated to be 40–50% by comparing the number of isolated nuclei to the starting cell number. Isolated nuclei were digested with Soluene-350 overnight. Hionic Fluor was added, and the radioactivity was determined using a liquid scintillation counter. The percentage of nuclear uptake of the TFO in the liver was calculated as % of total hepatic uptake.

Statistical Analysis. Data were expressed as the mean \pm standard deviation (SD). $P < 0.05$ was considered statistically significant. Statistics were calculated based on unpaired Student's *t* test using SPSS 13.0 for windows software.

RESULTS

To enhance the cellular uptake and nuclear translocation of the TFO, we conjugated M6P-BSA to the 3' end of the TFO via a disulfide bond. M6P-BSA-TFO was then characterized in terms of in vitro cellular and nuclear uptake and transcription inhibition of type $\alpha 1(\text{I})$ collagen gene in HSC-T6 cells. This was followed by biodistribution at whole body, organ (liver), and hepatic cellular and subcellular levels after intravenous injection into normal and fibrotic rats.

In Vitro Cellular and Nuclear Uptake of M6P-BSA-TFO. We have previously shown that M6P-BSA-TFO could enhance the TFO accumulation in the liver and thus concentrated TFO molecules inside HSCs compared to free TFO molecules (37). However, we still need to determine whether this enhanced TFO deposition is contributed to by an increase in M6P-BSA-TFO uptake by the HSCs via the M6P/IGF II receptor-mediated endocytosis. We first incubated HSC-T6 cells with ³³P-TFO or M6P-BSA-³³P-TFO for different time periods. As shown in Figure 1a, a larger amount of TFO was taken up by these cells when treated with M6P-BSA-³³P-TFO compared to that of ³³P-TFO treated cells. The TFO amount was around 1 ng/ μg of

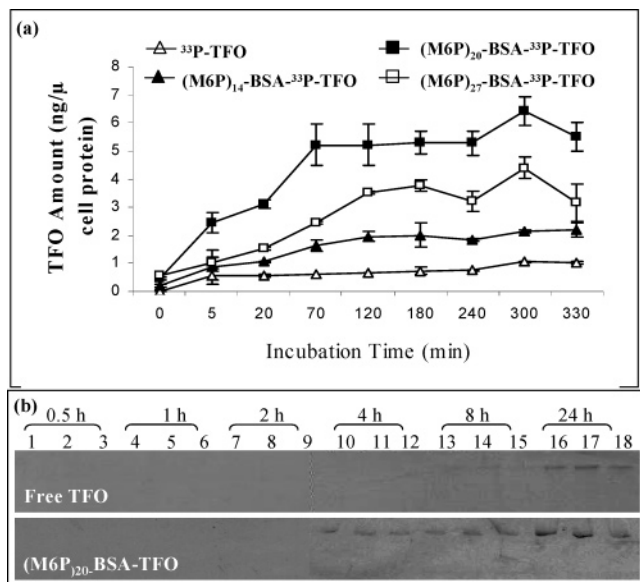


Figure 1. Cellular uptake of M6P-BSA-TFO by HSC-T6 cells. (a) Time profile of the cellular uptake of M6P-BSA- ^{33}P -TFO and ^{33}P -TFO by HSC-T6 cells. HSC-T6 cells were incubated with ^{33}P -TFO or M6P-BSA- ^{33}P -TFO (3×10^4 cpm, $0.4 \mu\text{M}$) at 37°C , and then cells were harvested at the indicated time for measurement of associated radioactivity. TFO concentration was expressed in terms of ng of TFO/ μg of cell protein. Values are mean \pm SD of 3 independent experiments. (b) Polyacrylamide gel electrophoresis (PAGE) of the TFO extracted from HSC-T6 cells. HSC-T6 cells were incubated with ^{33}P -TFO or (M6P) $_{20}$ -BSA- ^{33}P -TFO at 37°C for up to 24 h. Cells were harvested at the indicated time and lysed with 1% SDS lysis buffer. TFO was extracted and analyzed by gel electrophoresis using a 20% polyacrylamide gel. Each time point was presented with 3 independent experiments.

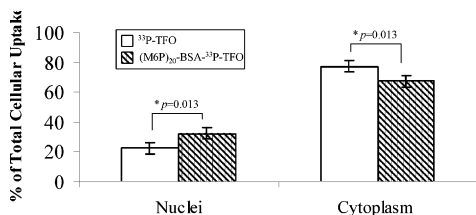


Figure 2. Subcellular distribution of (M6P) $_{20}$ -BSA- ^{33}P -TFO and ^{33}P -TFO in HSC-T6 cells at 4 h postincubation at 37°C . Cells were harvested and the nuclei were isolated from the cytoplasm using Nuclei EZ PREP nuclei isolation kit (Sigma, St Louis, MO). The subcellular distribution was expressed as % of total cellular uptake, and values are mean \pm SD of 3 independent experiments. Asterisk: statistically significant.

cell protein for unconjugated TFO. Conjugates with different numbers (x) of M6P residues ($x = 14, 20,$ and 27) showed different cellular uptake, with 2, 5, and 3 ng of TFO/ μg of cell protein, respectively. The optimal number of M6P for M6P-BSA-TFO is 20. The enhanced cellular uptake of the conjugates was also confirmed by polyacrylamide gel electrophoresis (Figure 1b). Bands clearly appeared at 4 h postincubation with (M6P) $_{20}$ -BSA- ^{33}P -TFO; however, the control TFO appeared only after 24 h of treatment. Moreover, the cellular uptake of M6P-BSA- ^{33}P -TFO was time dependent (Figure 1a,b).

Since the TFO molecules have to function inside the nucleus of the hepatic stellate cells by forming a triplex with the target genomic DNA sequence (22), we also determined the nuclear translocation of M6P-BSA- ^{33}P -TFO. As shown in Figure 2, relatively more TFO translocated into the nucleus ($\sim 32\%$ of total cellular uptake) in the case of (M6P) $_{20}$ -BSA- ^{33}P -TFO compared to nonconjugated TFO molecules ($\sim 23\%$ of total cellular uptake), possibly due to the efficient cellular uptake of M6P-BSA- ^{33}P -TFO by HSC-T6 cells.

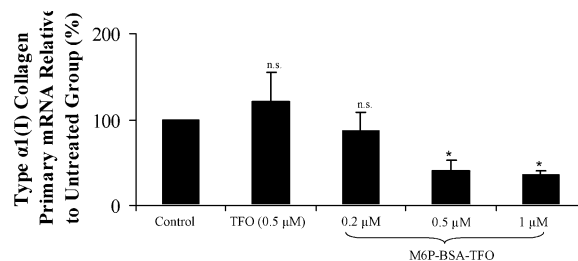


Figure 3. Relative type $\alpha 1(\text{I})$ collagen gene transcription in HSC-T6 cells treated with TFO or (M6P) $_{20}$ -BSA-TFO by real time RT-PCR assay. HSC-T6 cells were treated with unconjugated TFO ($0.5 \mu\text{M}$) or (M6P) $_{20}$ -BSA-TFO at the indicated concentrations in 1 mL of FBS-free DMEM for 24 h, and then 1 mL of DMEM containing 20% of FBS was added and incubated for another 24 h. Relative transcript levels were normalized using 18S rRNA as a housekeeping gene. Control means no treatment. Values are mean \pm SD of 3 independent experiments. Asterisk: statistically significant compared to control group. n.s.: not significant.

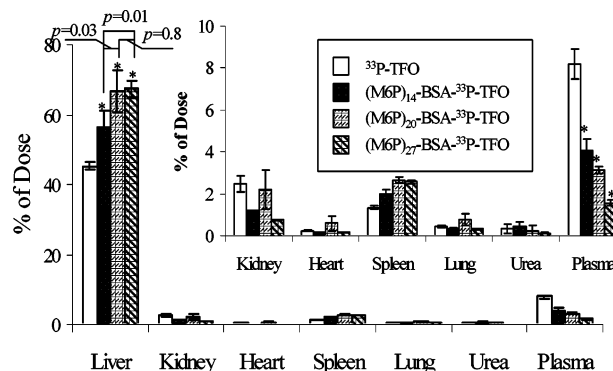


Figure 4. Effect of number of M6P per BSA on biodistribution of M6P- ^{33}P -BSA-TFO in normal rats. At 30 min postinjection of M6P-BSA- ^{33}P -TFO ($\sim 2.2 \times 10^5$ cpm) at a dose of 0.2 mg/kg , blood was collected by cardiac puncture and urine from the urinary bladder. Rats were sacrificed; major organs were isolated, washed with saline, blotted dry, and subjected to scintillation counting. Values are mean \pm SD of 4 rats in each group. Asterisk: statistically significant comparing to naked TFO group.

Inhibition of Type $\alpha 1(\text{I})$ Collagen Gene Transcription. Higher cellular uptake of M6P-BSA-TFO was expected to have higher efficiency in inhibiting the transcription of type $\alpha 1(\text{I})$ collagen gene. We used real time RT-PCR to quantify the primary mRNA levels. It was found that at the concentration of $0.5 \mu\text{M}$, free TFO molecules had no clear effect on the transcription inhibition. In contrast, for (M6P) $_{20}$ -BSA-TFO, we observed dose-dependent transcription inhibition. Transcription product was decreased to 87% of control group at $0.2 \mu\text{M}$, 40% at $0.5 \mu\text{M}$, and 35% at $1 \mu\text{M}$ (Figure 3).

Effect of Number of M6P on Biodistribution of M6P-BSA- ^{33}P -TFO. Since M6P is a ligand for the M6P/IGF II receptor expressed on the surface of the HSCs, the degree of M6P substitution per BSA molecule is likely to have a significant effect on the hepatic uptake and biodistribution of M6P-BSA- ^{33}P -TFO. Therefore, we determined the effect of the number of M6P per BSA on the biodistribution of M6P-BSA- ^{33}P -TFO. As shown in Figure 4, there was a significant increase in the amount of radioactivity in the liver compared to free TFO and as the number of M6P per BSA increased from 14 to 27, the hepatic uptake was 56.3%, 66.6%, and 67.4% for (M6P) $_{14}$ -BSA- ^{33}P -TFO, (M6P) $_{20}$ -BSA- ^{33}P -TFO, and (M6P) $_{27}$ -BSA- ^{33}P -TFO, respectively. However, no statistical difference was found between the (M6P) $_{20}$ - ^{33}P -TFO and (M6P) $_{27}$ - ^{33}P -TFO injected groups for the hepatic uptake (66.6% vs 67.4% of the injected dose). The amount of radioactivity in the spleen also increased (2.0%, 2.7%, and 2.6%, respectively) with increase in the number of M6P per BSA. In contrast, there was

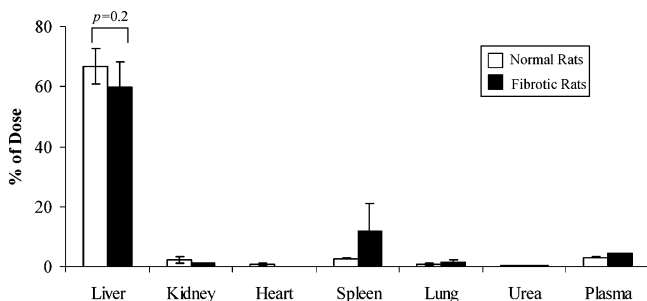


Figure 5. Effect of fibrosis on hepatic uptake of $(M6P)_{20}$ -BSA- ^{33}P -TFO after systemic administration into DMN-induced fibrotic rats. At 30 min postinjection of $(M6P)_{20}$ -BSA- ^{33}P -TFO ($\sim 2.2 \times 10^5$ cpm) at a dose of 0.2 mg/kg, blood was collected by cardiac puncture and urine from the urinary bladder. Rats were sacrificed; major organs were isolated, washed with saline, blotted dry, and subjected to scintillation counting. Values are mean \pm SD of 4 rats in each group.

a significant decrease in the plasma concentration compared to free TFO, and with increase in the number of M6P per BSA, the dose in the plasma was 4.1%, 3.1%, and 1.6%, respectively. The accumulation of different M6P-BSA-TFO in heart and lung was trivial. Since there was no significant difference in the hepatic uptake of $(M6P)_{20}$ -BSA- ^{33}P -TFO and $(M6P)_{27}$ -BSA- ^{33}P -TFO (Figure 4), we selected $(M6P)_{20}$ -BSA- ^{33}P -TFO for further studies.

Effect of Fibrosis on Biodistribution of M6P-BSA- ^{33}P -TFO. In the liver fibrosis process, activation of HSCs leads to accumulation of scar (fibril-forming) matrix, which in turn contributes to the loss of hepatocyte microvilli and sinusoidal fenestrae (2). These microstructural changes in the liver may prevent efficient drug delivery to HSCs.

We recently demonstrated that ^{33}P -TFO accumulation in the liver decreased from 43% in normal rats to 33% in fibrotic rats at 30 min postinjection (16). Therefore, we determined the biodistribution of $(M6P)_{20}$ -BSA- ^{33}P -TFO in DMN-induced liver fibrotic rats. As shown in Figure 5, there was no significant decrease in the hepatic uptake of $(M6P)_{20}$ -BSA- ^{33}P -TFO, which showed higher accumulation in both normal and fibrotic rats.

Competition in Hepatic Uptake of M6P-BSA-TFO. The role of M6P/IGF II receptor on biodistribution of M6P-BSA- ^{33}P -TFO in normal and fibrotic rats was assessed by determining the effect of excess M6P-BSA on the accumulation of M6P-BSA-TFO in the liver. By administration of excess M6P-BSA, the M6P/IGF II receptor can be saturated. Prior administration of M6P-BSA caused a significant decrease in the hepatic uptake of $(M6P)_{20}$ -BSA- ^{33}P -TFO at 30 min postinjection, suggesting the involvement of M6P/IGF II receptor in their hepatic uptake. The hepatic uptake of $(M6P)_{20}$ -BSA- ^{33}P -TFO decreased from 66.6% to 41.0% in the case of normal rats (Figure 6a), but from 59.7% to 14.3% in the case of fibrotic rats (Figure 6b). When we used BSA-TFO as a control, TFO accumulation in the liver was also significantly increased. However, there was only minimal decrease in its liver accumulation due to the prior injection of excess M6P-BSA (10 mg/kg), suggesting that its hepatic uptake is not mediated by M6P/IGF II receptor-mediated endocytosis (data not shown).

Hepatic Cellular and Subcellular Localization of M6P-BSA-TFO. Upregulation of M6P/IGF II receptors during fibrosis should increase M6P-BSA-TFO uptake by the HSCs and cancel out any adverse effect created by decreased sinusoidal gap. Therefore, the intrahepatic cellular localization of M6P-BSA-TFO was compared between normal and fibrotic rats, since HSCs are quiescent in normal rats, but get activated in fibrotic rats. The liver was perfused at 30 min post tail vein injection of $(M6P)_{20}$ -BSA- ^{33}P -TFO and ^{33}P -TFO as described before (16). Hepatocytes, Kupffer and endothelial cells, and

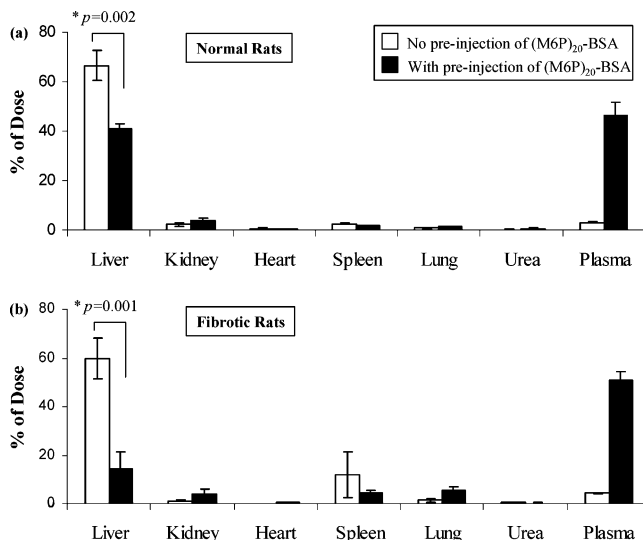


Figure 6. Inhibition of M6P-BSA on biodistribution of $(M6P)_{20}$ -BSA- ^{33}P -TFO in normal rats (a) and in fibrotic rats (b). $(M6P)_{20}$ -BSA (10 mg/kg) was injected intravenously into rats 5 min before the injection of $(M6P)_{20}$ -BSA- ^{33}P -TFO in normal and fibrotic rats at a dose of 0.2 mg/kg. At 30 min postinjection, rats were sacrificed; major organs were isolated, washed with saline, blotted dry, and subjected to scintillation counting. Values are mean \pm SD of 4 rats in each group. Asterisk: statistically significant.

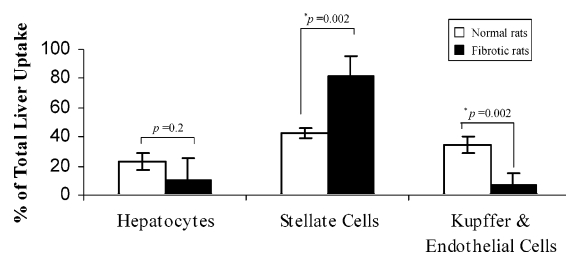


Figure 7. Intrahepatic distribution of $(M6P)_{20}$ -BSA- ^{33}P -TFO in normal and fibrotic rats. The liver was perfused in situ by collagenase/Pronase digestion after intravenous administration of ^{33}P -TFO or $(M6P)_{20}$ -BSA- ^{33}P -TFO at the dose of 0.2 mg of TFO/kg of body weight. Hepatocytes, Kupffer and endothelial cells, and stellate cells were separated, and the associated radioactivity was measured. The contribution of each cell type was expressed as % of total liver uptake. Values are mean \pm SD of 5 rats in each group. Asterisk: statistically significant.

HSCs were isolated, and the amount of radioactivity in these cells was determined. Figure 7 shows the percentages of contribution by different cell types in terms of total liver uptake of $(M6P)_{20}$ -BSA- ^{33}P -TFO after systemic administration in normal and fibrotic rats. In normal rats, 42.3% of total liver uptake was contributed by HSCs, 34.4% by Kupffer and endothelial cells, and 23.3% by hepatocytes. In contrast, in fibrotic rats, 82.0% of the total hepatic uptake was by HSCs, only 7.4% by Kupffer and endothelial cells, and 10.6% by hepatocytes. However, in the case of free TFO, there was not much difference for HSC contribution between normal and fibrotic rats (40% versus 44%) (16).

To study the subcellular distribution of the conjugate in vivo, we isolated the nuclei from rat liver at 30 min or 4 h after intravenous injection of $(M6P)_{20}$ -BSA- ^{33}P -TFO. Fractionation by sucrose gradient gave pure and intact nuclei (Figure 8), with a recovery of 40–50%. The majority of the TFO stayed in the cytoplasm of liver cells, and the TFO in the nuclei was only 4% of the total hepatic uptake at 30 min but increased up to 6% at 4 h. However, it is important to note that only half of the cell nuclei could be isolated. Therefore, the actual nuclear distribution of the TFO should be higher than this number.

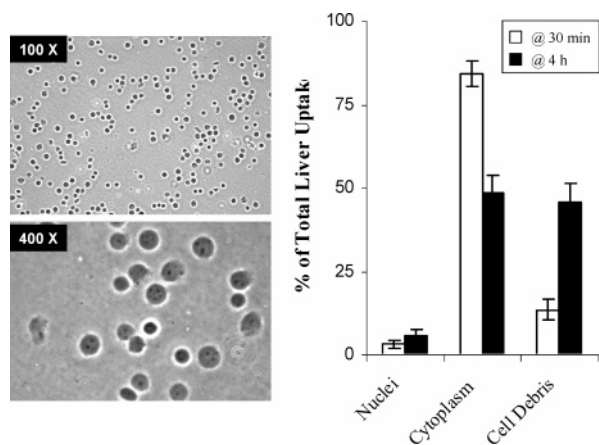


Figure 8. Subcellular distribution of $(M6P)_{20}$ -BSA- ^{33}P -TFO in the liver. At 30 min and 4 h after intravenous administration of $(M6P)_{20}$ -BSA- ^{33}P -TFO into normal rats at a dose of 0.2 mg/kg, rats were sacrificed and the livers were removed. The nuclei, cytoplasm, and cell debris were isolated from liver tissues using a sucrose gradient. Distribution in the nuclei, cytoplasm, and cell debris were given as % of the total liver uptake, and values are mean \pm SD of 4 rats in each group.

DISCUSSION

Fibrosis is characterized by excessive production of ECM composed primarily of type I collagen. Antisense ODNs have been shown to inhibit type $\alpha 1(I)$ collagen gene expression in NIH 3T3 cell in culture (23). Compared to quiescent HSCs, activated HSCs contain 60–70-fold more collagen $\alpha 1(I)$ mRNA (8, 24). Therefore, transfection of activated HSCs with molecular decoy and small interfering double stranded RNAs (siRNA) could significantly decrease $\alpha 1(I)$ collagen mRNA (24, 25). However, these authors did not attempt to deliver ODNs and siRNA to liver fibrogenic cells in vivo. Systemic administration of siRNA against Fas or Caspase 8 has shown some promise in controlling liver fibrosis (26, 27). However, these authors used high volume hydrodynamic administration, which is not feasible in a clinical setting. Moreover, siRNA is known to have an “off-target” effect.

To avoid the use of polycations, Rajur et al. (28) conjugated ODNs to asialoglycoprotein via a disulfide bond. Direct conjugation of molecules to the TFO often tends to disturb the triplex-forming ability of the TFOs, which is essential for transcription inhibition. In contrast, conjugation of M6P-BSA to TFO via a disulfide bond is stable in the circulation, but will be cleaved inside the cells by glutathione and/or redox enzymes. In the current study, we used a TFO molecule, which can specifically inhibit the transcription of type $\alpha 1(I)$ collagen gene by forming triplex at the promoter region (9, 29). One of the main advantages of the TFO over antisense ODNs and siRNA is that it targets two alleles of the target gene per cell rather than the mRNA, which is usually present in hundreds or thousands of copies per cell (22). After intravenous administration of the TFO, 35% of the injected dose accumulated in the liver of fibrotic rats and the intrahepatic distribution was nonspecific for HSCs (16).

M6P is a ligand for M6P/IGF II receptor, which is upregulated in fibroblast-like cells such as activated HSCs during liver fibrosis (18, 19). Coupling of M6P to albumin increased selective uptake of this modified albumin by HSCs during liver fibrosis (30). Conjugation of M6P to recombinant interleukin-10 (rIL-10) significantly increased the hepatic uptake of IL-10 by the liver. We synthesized M6P-BSA, conjugated to TFO via a disulfide bond, and determined the biodistribution of $(M6P)_{20}$ -BSA- ^{33}P -TFO after intravenous injection in normal rats (37). Significant increase in the hepatic uptake of the TFO

was observed. Since the hepatic uptake and bioactivity of $(M6P)_x$ -BSA-TFO are likely to be dependent on the dose and number of M6P per BSA, in this study, we synthesized $(M6P)_x$ -BSA-TFO, where $x = 14, 20,$ and 27 for both in vitro and in vivo studies.

HSC-T6 cell is a good cell culture system for studying the characteristics of activated HSCs in vitro (31). As shown in Figure 1, after conjugation with M6P-BSA, there was a significant increase in the TFO uptake by HSC-T6 cells. This is in a good agreement with the work of Bonfils et al. (32), who showed increased uptake of M6P-BSA-ODN by fibroblast-like BHK cells, which also expressed M6P/IGF II receptors. However, these authors had not tested their glycoconjugates in vivo. Also, $(M6P)_{20}$ -BSA-TFO gave the highest cellular uptake, so there was an optimal number of M6P attached to BSA (Figure 1a).

For triplex formation with genomic DNA, TFO must dissociate from M6P-BSA and translocate to the nucleus. TFO molecules were shown to be efficiently getting into the nucleus varying from 18.5% to 60.6% of total cellular uptake depending on different cell lines (33). We determined the nuclear uptake of $(M6P)_{20}$ -BSA- ^{33}P -TFO at 4 h postincubation to be around 32% and higher than that of ^{33}P -TFO in HSC-T6 cells (Figure 2). The increased nuclear translocation of the TFO was not expected, since there is no apparent reason for M6P-BSA-TFO to enhance the nuclear entry of the TFO molecules. The TFO was covalently conjugated with M6P-BSA via a disulfide bond, thus upon getting inside the cells, the disulfide bonds are expected to be cleaved and TFO molecules would enter the nucleus in an unconjugated form (37). So, this increased nuclear translocation of TFO molecules may be due to the relatively higher and faster cellular uptake of M6P-BSA-TFO by these cells than TFO alone, as shown in Figure 1. However, we observed a much less nuclear localization of $(M6P)_{20}$ -BSA- ^{33}P -TFO in vivo. It was only 4% at 30 min, but increased to 6% at 4 h (Figure 8). However, these values were underestimated since we could isolate only 40–50% of the nuclei from the liver tissue. The overall nuclear translocation of the TFO in the liver is likely to be as high as 15% at 4 h.

Previously, we have reported that the TFO can form triplex with the type $\alpha 1(I)$ collagen gene promoter sequence and inhibit the gene expression using a reporter plasmid containing the type $\alpha 1(I)$ collagen gene promoter sequence (9). However, we did not show direct inhibition of type $\alpha 1(I)$ collagen gene expression by the TFO. Since the half-life of type $\alpha 1(I)$ collagen mRNA is 20-fold longer in activated HSCs than that of quiescent HSCs (34), it is impossible to detect the effect of TFO at the mRNA level in cell culture. Therefore, we designed primers specific for type $\alpha 1(I)$ collagen primary mRNA to avoid this problem and demonstrated the gene inhibition effect of TFO. Higher cellular uptake was expected to have a more potent inhibitory effect on type $\alpha 1(I)$ collagen gene transcription. TFO molecules did not show any inhibitory effect at $0.5 \mu M$. In contrast, for M6P-BSA-TFO, we saw 60% inhibition at $0.5 \mu M$ and 65% at $1 \mu M$. Thus, M6P-BSA-TFO could efficiently increase the cellular uptake of TFO and also strengthen the TFO bioactivity.

The hepatic accumulation of M6P modified human serum albumin (M6P-HSA) was shown to be dependent on the number of M6P per HSA molecule and the highest hepatic accumulation and uptake by HSCs when HSA was substituted with 28 of M6P moieties (30). Therefore, we substituted 14, 20, and 27 M6P moieties per BSA for TFO delivery. As shown in Figure 4, the percentage of the injected dose accumulated in the liver significantly increased with increase in M6P density. Almost 56.3% of the injected dose was accumulated in the liver for $(M6P)_{14}$ -BSA-TFO, and an increase in the molar ratio of M6P:BSA to 27 resulted in an increased liver accumulation to

67.4%. Our results did not correlate well with the work of Beljaar et al. (30), who showed only a trivial accumulation of (M6P)_x-HSA in the liver when *x* was equal to 10 or below, but 59.2% as the hepatic uptake when *x* was equal to 28. This discrepancy is possibly due to the following two reasons: (i) we used M6P-BSA, since it was also shown that 52.6% accumulated in the liver for (M6P)₂₁-BSA (30); (ii) in our case, M6P-BSA was further conjugated with TFO, which is a polyanion with molecular weight of >8000Da, and must have some influence on the biodistribution of M6P-BSA. Apparently, there was a saturation in the hepatic uptake of M6P-BSA-TFO, since (M6P)₂₀-BSA-TFO and (M6P)₂₇-BSA-TFO were not significantly different in the hepatic uptake (Figure 4). This saturation was also observed for galactose modified BSA (Gal-BSA) by Staud et al. (35).

Since there is a concern that the fibrotic liver would prevent efficient drug delivery to the liver (30), we confirmed that there was no decrease in the hepatic uptake of (M6P)₂₀-BSA-TFO. This is in contrast to our recent findings on the biodistribution of ³³P-TFO, where we observed significant decrease in the hepatic uptake of ³³P-TFO when injected into fibrotic rats (16). This may be due to the fact that M6P/IGF II receptors are upregulated during fibrosis (18, 19), which should increase uptake by HSCs via receptor-mediated endocytosis and cancel out any adverse effect created by decrease in sinusoidal gap.

To determine whether the hepatic accumulation of M6P-BSA-³³P-TFO is mediated by M6P/IGF II receptor-mediated endocytosis, we preinjected rats with excess (M6P)₂₀-BSA. This resulted in a significant decrease in the hepatic disposition of M6P-BSA-³³P-TFO, and this decrease was even more significant in fibrotic rat liver (Figure 6). This confirmed the specific receptor-mediated uptake of M6P-BSA-³³P-TFO. When M6P/IGF II receptor was upregulated in fibrotic rats, the hepatic accumulation was almost completely inhibited by blocking this receptor. Rachmawati et al. also demonstrated almost 50% inhibition in the hepatic uptake of M6P-IL-10 conjugate in fibrotic rats (36).

Finally, we should make sure the conjugate was really targeted to HSCs. We observed that 42.3% of the hepatic uptake was in the HSCs of normal rats, but increased to 82.0% in the HSCs of fibrotic rats, which means (M6P)₂₀-BSA-TFO not only increased TFO accumulation in the liver in general but also specifically targeted to HSCs in fibrotic rats. At the same time, the contribution of Kupffer and endothelial cells was greatly inhibited compared to that in normal rats (7.4% vs 34.4%). Unconjugated TFO was mostly taken up by Kupffer and endothelial cells, possibly through the scavenger receptors (16). Thus, the biodistribution of TFO was changed by conjugation with M6P-BSA.

Although we isolated nuclei from the whole liver rather than from different isolated liver cells, we assume that the nuclear translocation of the TFO of different liver cells would be similar. Since most of the TFO accumulated in the HSCs of the fibrotic rats (Figure 7), we expect that TFO concentration inside the nuclei of HSCs would be much higher for M6P-BSA-TFO than that for free TFO and thus could greatly increase the potency of TFO molecules in vivo.

In conclusion, conjugation with M6P-BSA significantly enhanced the uptake of the TFO by HSCs both in vitro and in vivo. Therefore, M6P-BSA-TFO is a suitable delivery system for targeting TFO against type $\alpha 1(I)$ collagen gene promoter to HSCs for treating liver fibrosis.

ACKNOWLEDGMENT

This work was supported by Grant R01 DK064633 from the NIH and USPHS Grant 47379.

LITERATURE CITED

- (1) Kochanek, K. D., Murphy, S. L., Anderson, R. N., and Scott, C. (2004) Deaths: final data for 2002. *Natl. Vital Stat. Rep.* 53, 1–115.
- (2) Friedman, S. L. (2000) Molecular regulation of hepatic fibrosis, an integrated cellular response to tissue injury. *J. Biol. Chem.* 275, 2247–50.
- (3) Knittel, T., Kobold, D., Piscaglia, F., Saile, B., Neubauer, K., Mehde, M., Timpl, R., and Ramadori, G. (1999) Localization of liver myofibroblasts and hepatic stellate cells in normal and diseased rat livers: distinct roles of (myo-)fibroblast subpopulations in hepatic tissue repair. *Histochem. Cell Biol.* 112, 387–401.
- (4) Raghow, R. (1994) The role of extracellular matrix in postinflammatory wound healing and fibrosis. *FASEB J.* 8, 823–31.
- (5) Rockey, D. C. (2005) Antifibrotic therapy in chronic liver disease. *Clin. Gastroenterol. Hepatol.* 3, 95–107.
- (6) Maher, J. J. (2001) Interactions between hepatic stellate cells and the immune system. *Semin. Liver Dis.* 21, 417–26.
- (7) Wu, C. H., Walton, C. M., and Wu, G. Y. (2000) Targeted inhibition of type I procollagen synthesis by antisense DNA oligonucleotides. *Gene Ther. Regul.* 1, 193–205.
- (8) Stefanovic, B., Hellerbrand, C., Holcik, M., Briendl, M., Aliebbaber, S., and Brenner, D. A. (1997) Posttranscriptional regulation of collagen alpha1(I) mRNA in hepatic stellate cells. *Mol. Cell. Biol.* 17, 5201–9.
- (9) Joseph, J., Kandala, J. C., Veerapanane, D., Weber, K. T., and Guntaka, R. V. (1997) Antiparallel polypurine phosphorothioate oligonucleotides form stable triplexes with the rat alpha1(I) collagen gene promoter and inhibit transcription in cultured rat fibroblasts. *Nucleic Acids Res.* 25, 2182–8.
- (10) Sawai, K., Mahato, R. I., Oka, Y., Takakura, Y., and Hashida, M. (1996) Disposition of oligonucleotides in isolated perfused rat kidney: involvement of scavenger receptors in their renal uptake. *J. Pharmacol. Exp. Ther.* 279, 284–90.
- (11) Takakura, Y., Mahato, R. I., Yoshida, M., Kanamaru, T., and Hashida, M. (1996) Uptake characteristics of oligonucleotides in the isolated rat liver perfusion system. *Antisense Nucleic Acid Drug Dev.* 6, 177–83.
- (12) Agrawal, S., Tamsamani, J., and Tang, J. Y. (1991) Pharmacokinetics, biodistribution, and stability of oligodeoxynucleotide phosphorothioates in mice. *Proc. Natl. Acad. Sci. U.S.A.* 88, 7595–9.
- (13) Mahato, R. I., Takemura, S., Akamatsu, K., Nishikawa, M., Takakura, Y., and Hashida, M. (1997) Physicochemical and disposition characteristics of antisense oligonucleotides complexed with glycosylated poly(L-lysine). *Biochem. Pharmacol.* 53, 887–95.
- (14) Bijsterbosch, M. K., Manoharan, M., Dorland, R., Waarlo, I. H., Biessen, E. A., and van Berkel, T. J. (2001) Delivery of cholesteryl-conjugated phosphorothioate oligodeoxynucleotides to Kupffer cells by lactosylated low-density lipoprotein. *Biochem. Pharmacol.* 62, 627–33.
- (15) Bijsterbosch, M. K., Manoharan, M., Dorland, R., Van Veghel, R., Biessen, E. A., and Van Berkel, T. J. (2002) bis-Cholesteryl-conjugated phosphorothioate oligodeoxynucleotides are highly selectively taken up by the liver. *J. Pharmacol. Exp. Ther.* 302, 619–26.
- (16) Cheng, K., Ye, Z., Guntaka, R. V., and Mahato, R. I. (2005) Biodistribution and hepatic uptake of triplex-forming oligonucleotides against type alpha1(I) collagen gene promoter in normal and fibrotic rats. *Mol. Pharm.* 2, 206–17.
- (17) Beljaars, L., Olinga, P., Molema, G., de Bleser, P., Geerts, A., Groothuis, G. M., Meijer, D. K., and Poelstra, K. (2001) Characteristics of the hepatic stellate cell-selective carrier mannose 6-phosphate modified albumin (M6P(28)-HSA). *Liver* 21, 320–8.
- (18) de Bleser, P. J., Jannes, P., van Buul-Offers, S. C., Hoogerbrugge, C. M., van Schravendijk, C. F., Niki, T., Rogiers, V., van den Brande, J. L., Wisse, E., and Geerts, A. (1995) Insulinlike growth factor-II/mannose 6-phosphate receptor is expressed on CCl4-exposed rat fat-storing cells and facilitates activation of latent transforming growth factor-beta in cocultures with sinusoidal endothelial cells. *Hepatology* 21, 1429–37.
- (19) Weiner, J. A., Chen, A., and Davis, B. H. (1998) E-box-binding repressor is down-regulated in hepatic stellate cells during up-regulation of mannose 6-phosphate/insulin-like growth factor-II receptor expression in early hepatic fibrogenesis. *J. Biol. Chem.* 273, 15913–9.

- (20) Jenkins, S. A., Grandison, A., Baxter, J. N., Day, D. W., Taylor, I., and Shields, R. (1985) A dimethylnitrosamine-induced model of cirrhosis and portal hypertension in the rat. *J. Hepatol.* *1*, 489–99.
- (21) Jamall, I. S., Finelli, V. N., and Que Hee, S. S. (1981) A simple method to determine nanogram levels of 4-hydroxyproline in biological tissues. *Anal. Biochem.* *112*, 70–5.
- (22) Stull, R. A., and Szoka, F. C., Jr. (1995) Antigene, ribozyme and aptamer nucleic acid drugs: progress and prospects. *Pharm. Res.* *12*, 465–83.
- (23) Laptev, A. V., Lu, Z., Colige, A., and Prockop, D. J. (1994) Specific inhibition of expression of a human collagen gene (COL1A1) with modified antisense oligonucleotides. The most effective target sites are clustered in double-stranded regions of the predicted secondary structure for the mRNA. *Biochemistry* *33*, 11033–9.
- (24) Stefanovic, B., Schnabl, B., and Brenner, D. A. (2002) Inhibition of collagen alpha 1(I) expression by the 5' stem-loop as a molecular decoy. *J. Biol. Chem.* *277*, 18229–37.
- (25) Lindquist, J. N., Parsons, C. J., Stefanovic, B., and Brenner, D. A. (2004) Regulation of alpha1(I) collagen messenger RNA decay by interactions with alphaCP at the 3'-untranslated region. *J. Biol. Chem.* *279*, 23822–9.
- (26) Song, E., Lee, S. K., Wang, J., Ince, N., Ouyang, N., Min, J., Chen, J., Shankar, P., and Lieberman, J. (2003) RNA interference targeting Fas protects mice from fulminant hepatitis. *Nat. Med.* *9*, 347–51.
- (27) Zender, L., Hutker, S., Liedtke, C., Tillmann, H. L., Zender, S., Mundt, B., Waltemathe, M., Gosling, T., Flemming, P., Malek, N. P., Trautwein, C., Manns, M. P., Kuhnel, F., and Kubicka, S. (2003) Caspase 8 small interfering RNA prevents acute liver failure in mice. *Proc. Natl. Acad. Sci. U.S.A.* *100*, 7797–802.
- (28) Rajur, S. B., Roth, C. M., Morgan, J. R., and Yarmush, M. L. (1997) Covalent protein-oligonucleotide conjugates for efficient delivery of antisense molecules. *Bioconjugate Chem.* *8*, 935–40.
- (29) Nakanishi, M., Weber, K. T., and Guntaka, R. V. (1998) Triple helix formation with the promoter of human alpha1(I) procollagen gene by an antiparallel triplex-forming oligodeoxyribonucleotide. *Nucleic Acids Res.* *26*, 5218–22.
- (30) Beljaars, L., Molema, G., Weert, B., Bonnema, H., Olinga, P., Groothuis, G. M., Meijer, D. K., and Poelstra, K. (1999) Albumin modified with mannose 6-phosphate: A potential carrier for selective delivery of antifibrotic drugs to rat and human hepatic stellate cells. *Hepatology* *29*, 1486–93.
- (31) Vogel, S., Piantedosi, R., Frank, J., Lalazar, A., Rockey, D. C., Friedman, S. L., and Blaner, W. S. (2000) An immortalized rat liver stellate cell line (HSC-T6): a new cell model for the study of retinoid metabolism in vitro. *J. Lipid Res.* *41*, 882–93.
- (32) Bonfils, E., Depierreux, C., Midoux, P., Thuong, N. T., Monsigny, M., and Roche, A. C. (1992) Drug targeting: synthesis and endocytosis of oligonucleotide-neoglycoprotein conjugates. *Nucleic Acids Res.* *20*, 4621–9.
- (33) Cho, J. G., Kim, M. K., Oh, E. J., Yoon, E. J., Sohn, J., Park, M. K., and Park, G. H. (2002) Pharmacokinetics of (111)In-labeled triplex-forming oligonucleotide targeting human N-myc gene. *Mol. Cells* *14*, 93–100.
- (34) Sato, M., Suzuki, S., and Senoo, H. (2003) Hepatic stellate cells: unique characteristics in cell biology and phenotype. *Cell Struct. Funct.* *28*, 105–12.
- (35) Staud, F., Nishikawa, M., Takakura, Y., and Hashida, M. (1999) Liver uptake and hepato-biliary transfer of galactosylated proteins in rats are determined by the extent of galactosylation. *Biochim. Biophys. Acta* *1427*, 183–92.
- (36) Rachmawati, H. (2005) Chemically modified IL-10 with a liver-specific ligand: a new strategy for the treatment of liver fibrosis with a therapeutic cytokine. Ph.D. Thesis, 106–28.
- (37) Ye, Z., Cheng, K., Guntaka, R. V., and Mahato, R. I. (2005) Targeted Delivery of a Triplex-Forming Oligonucleotide to Hepatic Stellate Cells. *Biochemistry* *44*, 4466–76.

BC060006Z